TURBULENT FLOW FORCES ON HYDRAULIC VALVES: A PARALLEL VORTEX SIMULATION METHOD

Athanassios A. Dimas [1]
Krispin Technologies, Inc.
1370 Piccard Dr.
Rockville, Maryland 20850
Email: adimas@krispintech.com

Isaac Lottati
Krispin Technologies, Inc.
1370 Piccard Dr.
Rockville, Maryland 20850
Email: lottati@krispintech.com

Ronald H. Miller
Scientific Research Laboratory
Ford Motor Company
Dearborn, Michigan, 48121
Email: rmiller47@ford.com

Gary S. Strumolo
Scientific Research Laboratory
Ford Motor Company
Dearborn, Michigan, 48121
Email: gstrumol@ford.com

Peter S. Bernard
Department of Mechanical Engineering
University of Maryland
College Park, Maryland, 20742
Email: bernard@eng.umd.edu

ABSTRACT

The unique software VORCAT (VORtex Computational Algorithm for Turbulence), which is based on a fast parallel vortex method, is employed to perform a time-accurate simulation of the flow in the spool valve of a pressure regulator from an automotive automatic transmission. The spool valve experiences flow forces which affect its axial motion and radial clearance. The vortex method is based on a parallel implementation of the Fast Multipole Method, and includes a hybrid vortex filament/sheet representation of the flow field, a vortex filament creation model that imitates the physical vortex self-replication process, and a hairpin removal and reconnection mechanism to limit the number and scale of vortical structures to those that are dynamically essential. In this paper, velocity and vorticity distribution results are presented for spool valve openings of 1mm and 0.25mm. The predicted velocity results agree well with corresponding experimental measurements, while the predicted vorticity results correlate well with experimental pressure measurements.

INTRODUCTION

Many mechanical systems employing fluid power use one or more spool-type hydraulic valves to control fluid flow. One such system is an automatic transmission system whose hydraulic circuit involves many inlets and exits, reversing flow, flow and pressure controls, and many other unique features that add complexity to the flow dynamics. The spool valve experiences inertial, frictional and flow forces which affect its axial motion and radial clearance. Flow forces are hard to model since their magnitude depends on operating conditions and valve geometry which, subsequently, regulate the fluid flow rate. Non-dimensional analytical approximations to the flow force exist for simplified geometries; however, for complex three-dimensional valve designs, the determination of flow forces requires either experimental data or three-dimensional computational analysis. With an accurate description of the flow force, not only can leakage and wear issues be potentially identified, but control strategies for transmission operation can be determined. It also assists in geometry optimization aimed at reducing undesirable flow force effects.

In this paper, the unique software VORCAT (VORtex Computational Algorithm for Turbulence), which is based on a fast parallel vortex method, is employed to perform a time-accurate simulation of the flow in a pressure regulator spool valve from an automotive automatic transmission. A cross-section of the valve is shown in Figure (1). Detailed flow field information are calculated for orifice openings of 1mm and 0.25 mm and compared to available experimental data. In the next section, a brief description of the VORCAT methodology is presented.

[1] Address all correspondence to this author.

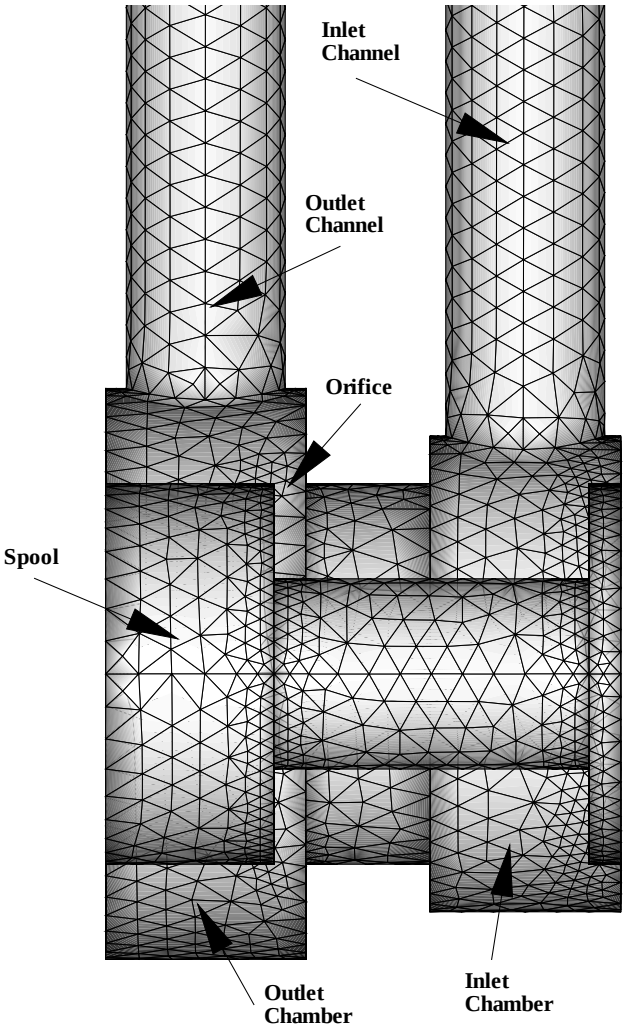

Figure 1. CROSS-SECTION OF THE SPOOL-TYPE VALVE WITH AN ORIFICE OPENING OF 1mm. THE INLET AND OUTLET CHANNELS HAVE DIAMETERS OF 5mm.

VORCAT METHODOLOGY

In VORCAT, as in all vortex methods, the evolution of the vorticity field, $\mathbf{\Omega}(\mathbf{x},t)$, in three-dimensional flow is governed by the transport equation

$$\frac{\partial \mathbf{\Omega}}{\partial t} + (\nabla \mathbf{\Omega})\mathbf{u} = (\nabla \mathbf{u})\mathbf{\Omega} + \frac{1}{R}\nabla^2 \mathbf{\Omega} \qquad (1)$$

where $\mathbf{u}$ is the velocity field and R is the Reynolds number. In vortex methods (Puckett, 1993), numerical solutions to (1) are obtained in the form of collections of N_v vortex elements covering the support of the vorticity field. In the case of turbulent flow, it is most convenient to use a combination of smoothed vortex sheets and vortex filaments near solid boundaries, while filaments are used exclusively elsewhere (Bernard, 1995; Bernard, 1999; Bernard, 1999). In view of the linear dependence of (1) on vorticity, there is little difficulty in accommodating the coexistence of sheets and filaments near solid walls.

Sheets arrayed in thin layers provide an efficient means for capturing wall-normal viscous diffusion, which is significant only near walls for high Reynolds number flows. In VORCAT, the sheets are in the form of an unstructured triangularization over several parallel layers (Bernard, 1999).. This is well tuned to capturing the complex geometrical features found in many applied problems but without the onerous task of devising a grid to cover the entire flow domain. The use of thin vortex sheets in a fixed array allows for the use of an accurate finite volume solution of equation (1).

The vortex filaments provide a natural means for representing the vortical structures – coherent or otherwise – which play a major role in the dynamics of turbulent flow (Bernard, 1993; Panton, 1997). The filament part of the calculation is adapted directly from standard grid-free schemes using collections of tubes (Chorin, 1993). Each filament (which may be composed of a number of straight-line segments) is assigned a constant circulation along its length. A fractional step method is used to solve (1) in Lagrangian form for the filaments. The end points, $\mathbf{x}_i(t)$, of each segment are moved in time according to a discretization of the kinematic equation, $d\mathbf{x}_i/dt = \mathbf{u}(\mathbf{x}_i(t),t)$, which accounts for both the stretching and convection terms.

Following the approach of Chorin (1993), folded vortex segments forming hairpins are removed when their interior angle is less than a critical angle. This step is tantamount to a physically based subgrid re-normalization limiting resolution to just the larger scales. Vortex destruction is accommodated in two different ways (Bernard, 1999; Bernard, 1999). In the first, vortices are eliminated if they become overly stretched, i.e. are formed from a large number of filament segments. Such older structures tend to be chaotic and their removal paves the way for relatively young, more coherently organized vortices to dominate the flow. In the second, vortices, which are not being sufficiently stretched, are allowed to lose an appropriate amount of circulation at each time step, specifically, that amount which would diffuse beyond their core radius. Vortices whose circulations drop below a threshold can then be eliminated.

Providing for each new generation of vortex tubes as they are produced in a turbulent flow is also a critical aspect of the numerical scheme. The algorithm must at the same time be both sensitive to the physical process by which new structures appear, yet not so unconstrained as to allow for the formation of impossibly large numbers of new vortices. A successful means of accommodating these conditions has

been developed (Bernard, 1999). Specifically, sheet vorticity above a critical threshold at the end of the sheet domain is reformulated into filaments. This models the process by which parent quasi-streamwise vortices provoke the creation of counter-rotating offspring through ejection and subsequent reorientation of the spanwise vorticity produced at the boundary in fulfillment of the no-slip condition. As shown in (Bernard, 1999), this algorithm successfully maintains a population of parent quasi-streamwise vortices near solid boundaries.

The velocity field is computed as a sum of the contributions from individual elements using the Biot-Savart law (Puckett, 1993). For the ith tube segment, the smoothed velocity field induced at a point $\mathbf{x}$ is computed from

$$-\frac{\Gamma_i}{4\pi}\frac{\mathbf{r}_i \times \mathbf{s}_i}{\mid \mathbf{r}_i \mid^3}\phi(r/\sigma) \qquad (2)$$

where Γ_i is the circulation, $\mathbf{r}_i = \mathbf{x}_i - \mathbf{x}$, $r = \mid \mathbf{r} \mid$, $\phi(r) = 1 - \left(1 - \frac{3}{2}r^3\right)e^{-r^3}$ is a higher order smoothing function, $\mathbf{s}_i$ is the axial vector along the segment and σ is a scaling parameter. In the case of sheets, the velocity field due to the ith sheet may be determined from the smoothed Biot-Savart integral in the form

$$\int_{V_i} K_\eta(\mathbf{x} - \mathbf{x}')\mathbf{\Omega}(\mathbf{x}', t)d\mathbf{x}' = \mathbf{A}(\mathbf{x} - \mathbf{x}_i) \times \mathbf{\Omega}_i \qquad (3)$$

where V_i is the volume of the sheet, K_η is a smoothed form of the Biot-Savart kernel, and the vector field $\mathbf{A}(\mathbf{x})$ is computable in closed form from integrals of K_η. A piecewise linear vorticity distribution is assumed over each sheet. Then, the velocity field due to a collection of sheets and filaments is the sum of the individual contributions.

Vortex method computations of three-dimensional flows in complex geometries require the use of a large number, N_v, of vortex elements in order to adequately resolve the vortical flow processes which are critical to accurately modeling turbulent flow. The practical implementation of vortex methods depends on the fast computation of the nominally $O(N_v N_f)$ operations, implicit in the direct computation of velocities induced by N_v vortex elements on N_f field points, because this is the most time-consuming operation. In most implementations of vortex methods, including ours, $N_f \approx N_v$, hence the operations in the direct velocity computation are of $O(N_v^2)$. To reduce the cost of this operation, the fast multipole method (FMM) (Carrier et al., 1988; Greengard and Rokhlin, 1987; Strickland and Baty, 1993) is employed, which is a fast summation scheme for calculating velocities produced by a large number of vortons. In three dimensions, the FMM combines the velocity field induced by collections of nearby vortices into a single local expansion in spherical harmonics. By shifting the center of the expansion to the neighborhood of other collections of vortices, an efficient velocity field calculation can be effected. With use of an oct-tree structure to efficiently group vortices into near and well separated boxes, an $O(N_v \log N_v)$ algorithm results. VORCAT employs a parallel implementation of the FMM algorithm (Collins et al., 1999) which significantly reduces calculation time.

RESULTS

The flow through the spool valve configuration described in the introduction was studied for three conditions: (1) flow with an orifice opening of 1mm, (2) flow with an orifice opening of 0.25mm, and (3) reverse flow with an orifice opening of 1mm. In the reverse flow conditions, fluid enters from the outlet channel and exits from the inlet channel. In all cases, the influx rate is 40l/min resulting in an average influx velocity of 34m/s. The Reynolds number based on the average influx velocity and the inlet/outlet channel diameter of 5mm is 8833. The triangularization of all the valve surfaces consists of about 8500 triangles as shown in Figure (1). All computations were performed on an Origin2000 and a T3E, both machines belonging to the Cray Corporation. The computational time was about 20 secs per time on 32 Origin2000 processors, and about 1 min per time step on 32 T3E processors. Each run required about 8,000 time steps for the flow to reach a non-dimensional time of 2.

Velocity field vector plots and spanwise vorticity contour plots for all flow conditions are shown in Figures (2) - (9). The velocity vectors are shown at a distance of 0.075mm normal to the wall surface, while the vorticity contours are at the wall surface.

The regular flow conditions are characterized by strong spanwise vorticity formed on the outer edge of the outlet side of the spool (Figures (3) and (5)) for both valve openings. The velocities through the orifice opening (Figures (6) and (7)) are higher in the 0.25mm case, as expected, resulting in higher vorticity values as well, compared to the 1mm case. For the 0.25mm case, our computational prediction for a maximum non-dimensional velocity of 2.86 (dimensional velocity of 97.3m/s) in the orifice agrees well with the experimental measurement of 99.9m/s (Sumita and Kobayashi). On the inlet side, there is not any significant spanwise vorticity formation on the spool (Figures (2) and (4)) for both valve openings. According to an integral formulation theory by Uhlman (1992), the surface pressure distribution correlates with the vorticity distribution. Measurements of the pressure on the inlet and outlet spool surfaces (Sumita

and Kobayashi) exhibit the same distribution with the computed spanwise vorticity. Currently, the above mentioned integral formulation by Uhlman (1992) is adopted in order to develop a pressure solver capability for VORCAT.

In the 1mm case, there is a recirculation zone between the outer edge of the inlet side of the spool and the chamber walls (Figure (2)) due to the significant intrusion of the spool in the chamber. In the 0.25mm case (Figure (4)), there is no recirculation zone.

The reverse flow conditions are characterized by strong spanwise vorticity formed on the outer edges of the inlet side of the spool (Figure (8)) which is the outflow in this configuration.

CONCLUSION

The processes of transmission design and calibration as well as wear studies, require component testing which can be costly and time consuming. Through numerical simulations this time can be significantly reduced while addressing design sensitivity on flow induced forces, leakage, and wear issues. The simulations presented in this paper represent one such methodology aimed at enhancing transmission operation and design through numerical simulation.

ACKNOWLEDGMENT

This work was supported in part by the Ford Motor Company; the authors are grateful to C. Wu and I. Salmeen for their support. Computer time on the Origin2000 and T3E was provided by the CFD Group of Cray; the authors are grateful to J. Dawson for his support.

REFERENCES

Bernard, P. S., 1995, "A Deterministic Vortex Sheet Method for Boundary Layer Flow," *J. Comput. Phys.*, Vol. 117, pp. 132-145.

Bernard, P. S., 1999, "Toward a Vortex Method Simulation of Non-Equilibrium Turbulent Flows," In *Modeling Complex Turbulent Flows*, M.D. Salas et al., Kluwer Academic Pub., pp. 161 - 181.

Bernard, P. S., Dimas, A. A., and Lottati, I., 1999, "Vortex Method Analysis of Turbulent Flows," *Proc. First International Conference on Vortex Methods* **ICVM/99**, pp. 137-155, Kobe, Japan.

Bernard, P. S., Thomas, J. M., and Handler. R. A., 1993, "Vortex Dynamics and the Production of Reynolds Stress," *J. Fluid Mech.*, Vol. 253, pp. 385 - 419.

Carrier, J., Greengard, L., and Rokhlin, V., 1988, "A Fast Adaptive Multipole Algorithm for Particle Simulations," *SIAM J. Sci. Stat. Comput.*, Vol. 9, pp. 669-686.

Chorin, A. J., 1993, "Hairpin Removal in Vortex Interactions II," *J. Comput. Phys.*, Vol. 107, pp. 1-9.

Collins, J. P., Dimas, A. A., and Bernard, P. S., 1999, "A Parallel Adaptive Fast Multipole Method for High Performance Vortex Method Based Simulations," *Proc. ASME Fluids Engineering Division*, Vol. 250, pp. 307-314, Nashville, Tennessee.

Greengard, L., and Rokhlin, V., 1987, "A Fast Algorithm for Particle Simulations," *J. Comput. Phys.*, Vol. 73, pp. 325-348.

Panton, R. L., ed., 1997, "Self-Sustaining Mechanisms of Wall Turbulence," *Advances in Fluid Mechanics*, Vol. 15, Computational Mechanics Publications.

Puckett, E. G., 1993, "Vortex Methods: An Introduction and Survey of Selected Research Topics," In *Incompressible Computational Fluid Dynamics: Trends and Advances*, M. D. Gunzburger and R. A. Nicolaides, ed., Cambridge University Press, pp. 335-407.

Strickland, J. H., and Baty, R. S., 1993, "A Three Dimensional Fast Solver for Arbitrary Vorton Distributions," *Technical Report SAND93-1641*, Sandia National Laboratories.

Sumita, T., and Kobayashi, T., "A Numerical Study of Flow in a Spool Valve," Article in Japanese, pp. 482-484.

Uhlman Jr., J. S., 1992, "An integral equation formulation of the equations of motion of an incompressible fluid," NUWC-NPT Technical Report 10086, Naval Undersea Warfare Center Division, Newport, Rhode Island.

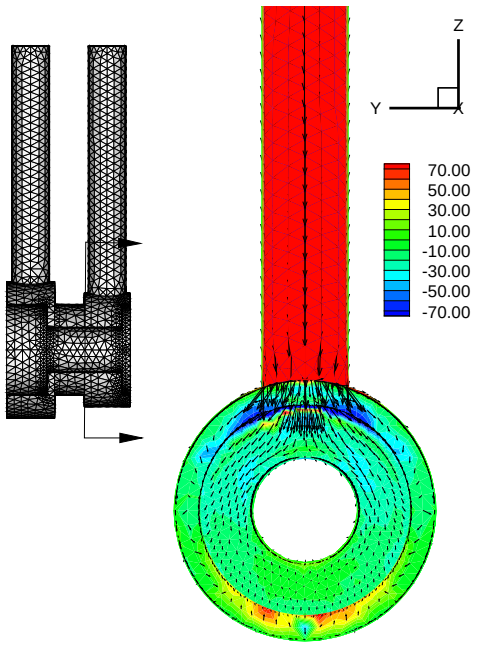

Figure 2. VELOCITY VECTOR FIELD AND SPANWISE VORTICITY DISTRIBUTION IN THE INLET CHANNEL AND SPOOL SURFACE FOR AN ORIFICE OPENING OF 1mm IN REGULAR FLOW CONDITION.

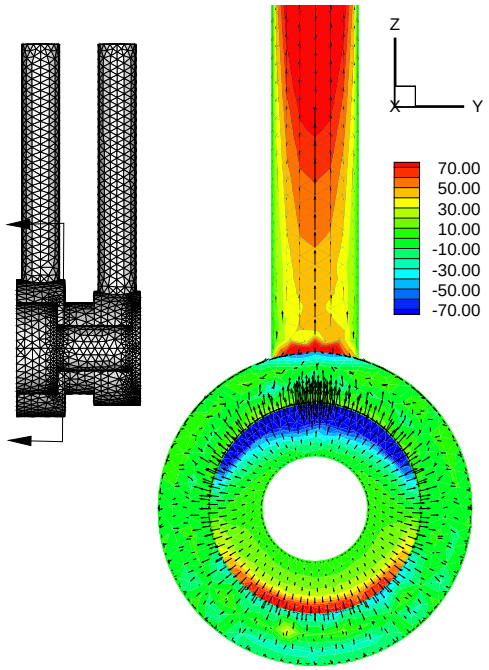

Figure 3. VELOCITY VECTOR FIELD AND SPANWISE VORTICITY DISTRIBUTION IN THE OUTLET CHANNEL AND SPOOL SURFACE FOR AN ORIFICE OPENING OF 1mm IN REGULAR FLOW CONDITION.

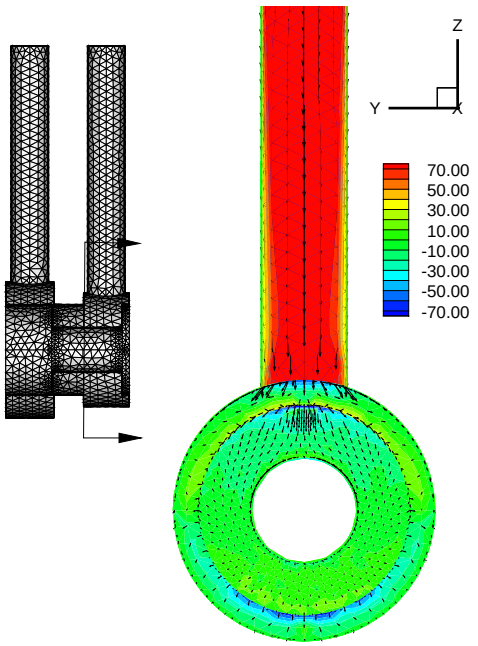

Figure 4. VELOCITY VECTOR FIELD AND SPANWISE VORTICITY DISTRIBUTION IN THE INLET CHANNEL AND SPOOL SURFACE FOR AN ORIFICE OPENING OF 0.25mm IN REGULAR FLOW CONDITION.

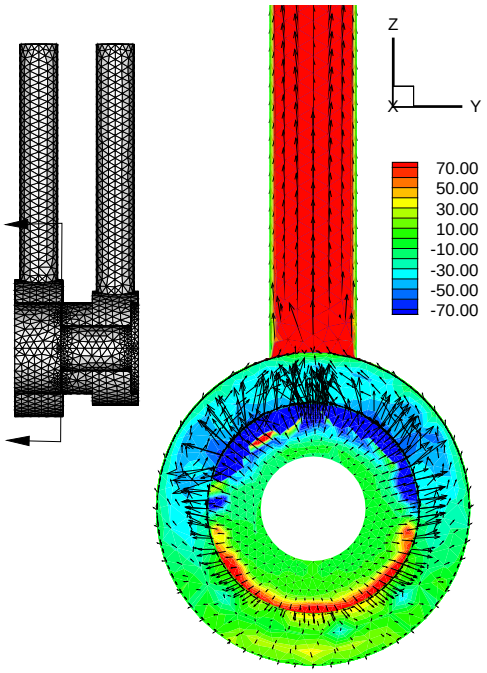

Figure 5. VELOCITY VECTOR FIELD AND SPANWISE VORTICITY DISTRIBUTION IN THE OUTLET CHANNEL AND SPOOL SURFACE FOR AN ORIFICE OPENING OF 0.25mm IN REGULAR FLOW CONDITION.

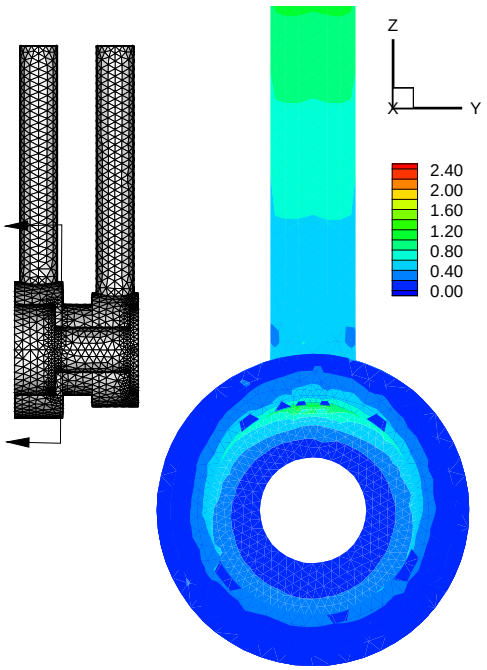

Figure 6. VELOCITY MAGNITUDE DISTRIBUTION IN THE OUTLET CHANNEL AND SPOOL SURFACE FOR AN ORIFICE OPENING OF 1mm IN REGULAR FLOW CONDITION.

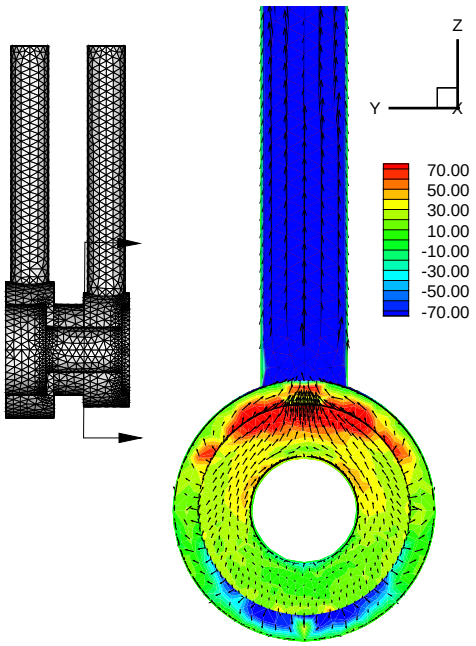

Figure 8. VELOCITY VECTOR FIELD AND SPANWISE VORTICITY DISTRIBUTION IN THE INLET CHANNEL AND SPOOL SURFACE FOR AN ORIFICE OPENING OF 1mm IN REVERSE FLOW CONDITION.

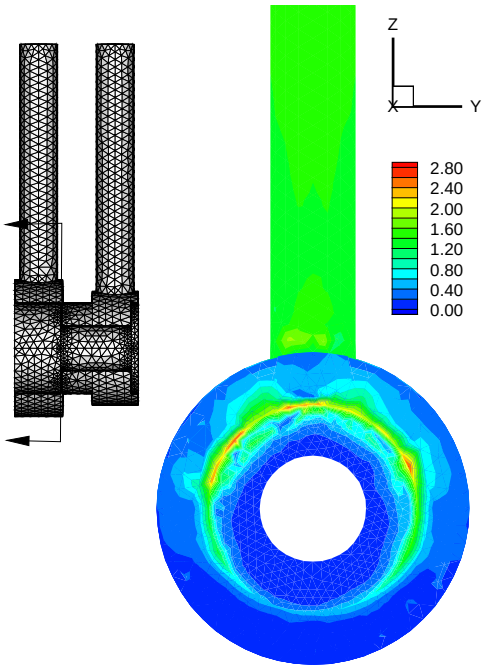

Figure 7. VELOCITY MAGNITUDE DISTRIBUTION IN THE OUTLET CHANNEL AND SPOOL SURFACE FOR AN ORIFICE OPENING OF 0.25mm IN REGULAR FLOW CONDITION.

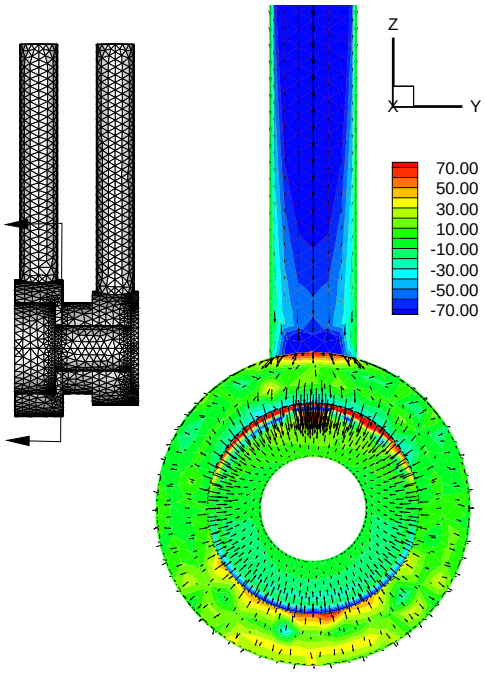

Figure 9. VELOCITY VECTOR FIELD AND SPANWISE VORTICITY DISTRIBUTION IN THE OUTLET CHANNEL AND SPOOL SURFACE FOR AN ORIFICE OPENING OF 1mm IN REVERSE FLOW CONDITION.